

In the (Very) Long Run We Are All Dead: Activation and Termination in SET-LRP/SARA-ATRP

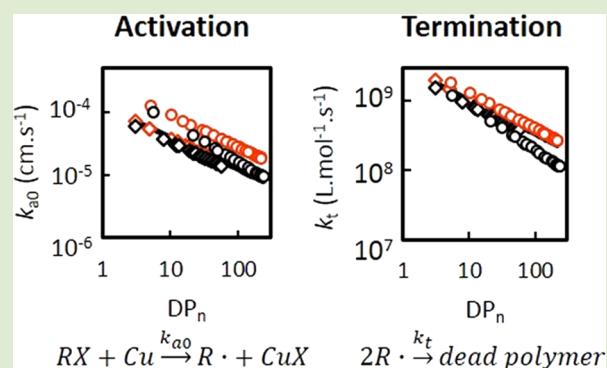
Simon Harrisson*[†] and Julien Nicolas[‡]

[†]IMRCP, UMR CNRS 5623, Université de Toulouse, 118 route de Narbonne, 31062 Toulouse Cedex 9, France

[‡]Institut Galien Paris-Sud, Univ Paris-Sud, UMR CNRS 8612, Faculté de Pharmacie, 5 rue Jean-Baptiste Clément, F-92296 Châtenay-Malabry Cedex, France

S Supporting Information

ABSTRACT: The rate constants of activation and termination were determined for SET-LRP/SARA-ATRP polymerizations of methyl acrylate. Measurement of the rate of generation of CuBr₂ throughout the reaction (using data from Levere et al., *Macromolecules* **2012**, *45*, 8267–8274) allowed evaluation of the chain length dependence of the two rate constants, which were found to be $1.25(9) \times 10^{-4} \text{DP}_n^{-0.51(3)} \text{ cm}\cdot\text{s}^{-1}$ (activation) and $3.1(1) \times 10^9 \text{DP}_n^{-0.49(2)} \text{ L}\cdot\text{mol}^{-1}\cdot\text{s}^{-1}$ (termination). Addition of the CuBr₂ deactivator at the beginning of the reaction is found to result in a higher proportion of dead chains due to rapid termination of short chains.



In a recent publication,¹ Percec and co-workers used UV–vis spectroscopy to measure the generation of CuBr₂ during polymerization of methyl acrylate (MA) initiated by methyl bromopropionate (MBP) and catalyzed by activated copper wire. Four polymerizations were carried out, using low (60/1) and high (222/1) ratios of MA/MBP and in the presence or absence of initial added CuBr₂. A monotonic increase in CuBr₂ concentration was observed, from which it was deduced that CuBr₂ is not reduced to CuBr. These experiments generated accurate kinetic data which we will make use of in this communication to shed light on activation and termination processes in reversible deactivation radical polymerization² in the presence of copper(0), known variously as SET-LRP^{3,4} or SARA-ATRP.⁵

Introduced by Percec et al. in 2002,⁶ and expanded to acrylates and methacrylates in 2006,⁷ SET-LRP is a type of reversible deactivation living radical polymerization in which radicals are initially generated by the reaction of an activated alkyl halide (typically an alkyl bromide) with copper metal in the form of wire, powder, or a colloidal suspension generated by in situ disproportionation of CuBr. Deactivation occurs, as in atom transfer radical polymerization (ATRP), by reaction of the propagating radicals with CuBr₂, forming a dormant polymer chain and CuBr.

The fate of the CuBr generated in the activation and deactivation steps has been the subject of controversy. According to one interpretation (SET-LRP),³ the CuBr instantaneously disproportionates to form CuBr₂ and nanoparticles of copper(0). The nanoparticulate copper is a highly reactive activator, while disproportionation of CuBr provides a source of deactivator which does not involve bimolecular

termination or the persistent radical effect, the main source of CuBr₂ in classical ATRP polymerizations. This has led to claims that SET-LRP polymerizations proceed without any bimolecular termination,^{8,9} supported by kinetic data showing that a polymerization which has been interrupted by removal of the copper wire recommences at an identical rate when the copper wire is reintroduced^{10,11} and by NMR and MALDI data showing complete^{1,4,9,12–14} or nearly complete^{15–19} retention of chain end functionality even at high conversions. The latter feature has allowed the preparation of complex multiblock architectures with high fidelity, either using sequential SET-LRP polymerizations^{15,16,18} or by SET-nitroxide radical coupling (SET-NRC).^{20–26}

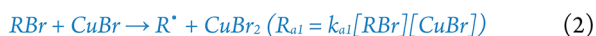
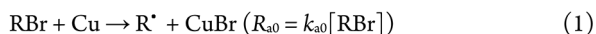
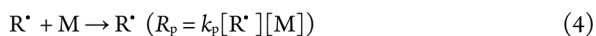
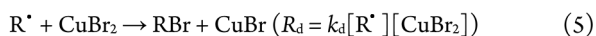
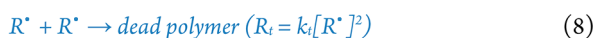
A second interpretation (SARA-ATRP)^{5,27–37} is that the copper acts as a supplemental activator and reducing agent (SARA). In this scheme, Cu^I (specifically [Cu^IL]⁺, where L represents the ligand),³⁸ not Cu⁰, is the major activating species, and Cu⁰ reduces Cu^{II} to Cu^I through comproportionation. Activation of dormant polymer chains by Cu⁰ occurs at a slow rate throughout the polymerization, and disproportionation is negligible. The key reactions of both mechanisms are summarized in Scheme 1.

In our own work on this polymerization,^{39–42} we have assumed that these interpretations are not totally incompatible: that *both* CuBr and Cu are activating species and that disproportionation *and* comproportionation take place concurrently, with one or the other predominating depending on

Received: May 20, 2014

Accepted: June 11, 2014

Published: June 16, 2014

Scheme 1. Dominant reactions in SARA-ATRP (Blue Italic)/SET-LRP (Red Underlined)^{a,b}
Activation**Propagation****Deactivation****Disproportionation/Comproportionation****Termination**

^aReactions common to both mechanisms are shown in black. ^bNote: RBr and R* represent dormant and active species, respectively. No distinction is made between initiator and polymer species in this simplified reaction scheme. CuBr and CuBr₂ represent all dissolved Cu^I and Cu^{II} species, respectively, and the corresponding rate constants represent weighted averages of the individual rate constants for each species. Cu* represents highly reactive nanosized copper ($k_{a0}^* \gg k_{a0}$).

the value of the disproportionation equilibrium constant and the concentrations of CuBr and CuBr₂. Using this approach, we developed a kinetic scheme for the polymerization which explains the observed 1/2-order dependence on initiator concentration and copper surface area.³⁹

Numerous experimental observations have shown that the reaction rapidly reaches a steady state, in which the concentration of radicals, [R*], is constant (denoted by [R*]_{SS}), leading to linear first-order kinetics across a large range of conversions. The rate of termination can be related to the rates of generation of CuBr and CuBr₂ by the following equations³⁹

$$\frac{d[R^*]}{dt} = \frac{d[CuBr]}{dt} + 2\frac{d[CuBr_2]}{dt} - 2k_t[R^*]_{SS}^2 = 0 \quad (9)$$

$$\frac{d[CuBr_2]}{dt} = k_t[R^*]_{SS}^2 - 0.5 \times \frac{d[CuBr]}{dt} \quad (10)$$

This relationship holds regardless of whether comproportionation or disproportionation predominates in the reaction mixture.

The concentration of CuBr₂ as a fraction of all dissolved copper species approaches φ ,³⁹ given by

$$\varphi = \frac{k_{a1}[RBr] + k_{disp}[CuBr]}{k_d[R^*] + k_{a1}[RBr] + k_{disp}[CuBr]}, \quad 0 < \varphi < 1 \quad (11)$$

For highly active catalysts ($k_{a1}[RBr] \gg k_d[R^*]$) such as CuBr/Me₆TREN in DMSO,⁴³ $\varphi \approx 1$, and negligible amounts of CuBr are generated during the reaction. Hence, to a good approximation, the rate of termination is given by the rate of generation of CuBr₂.⁴⁴

$$\frac{d[CuBr_2]}{dt} \approx k_t[R^*]^2 \quad (12)$$

As essentially all soluble copper is present in the form of CuBr₂, the rate of generation of CuBr₂ is also equal to the rate of activation by copper metal (assuming negligible comproportionation)

$$\frac{d[CuBr_2]}{dt} \approx (k_{a0}[RBr] + k_{comp}[CuBr_2])\frac{SA_{Cu}}{V} \quad (13)$$

$$\approx k_{a0}[RBr]\frac{SA_{Cu}}{V} \quad (14)$$

In eqs 13 and 14, SA_{Cu}/V represents the ratio of copper surface area to reaction volume.

Finally the rate of loss of chain end functionality occurs at twice the rate of CuBr₂ generation and is given by

$$-\frac{d[RBr]}{dt} = 2k_t[R^*]^2 \approx 2\frac{d[CuBr_2]}{dt} \quad (15)$$

This relationship allows the calculation not only of the total loss of functionality during polymerization, as has been carried out by Matyjaszewski et al. for various ATRP systems,⁴⁴ but also of the rate constants of activation by copper metal (k_{a0}) and bimolecular termination (k_t) throughout the polymerization.

Figure 1 (adapted from Figure 7 in ref 1) shows the evolution of the concentration of CuBr₂ during polymerizations

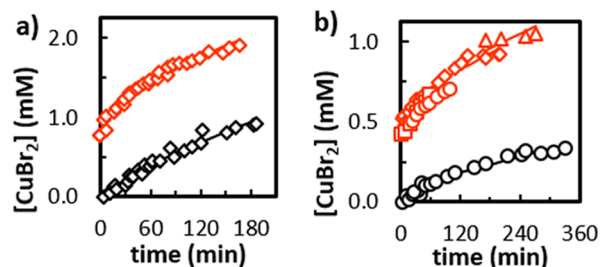


Figure 1. Variation of [CuBr₂] with time in polymerizations of MA initiated by MBP in the presence (red) or absence (black) of externally added CuBr₂ (adapted with permission from Levere, M. E.; Nguyen, N. H.; Percec, V. *Macromolecules* 2012, 45, 8267–8274. Copyright 2012 American Chemical Society).¹ [MA]₀/[MBP]₀ = 60/1 (a) or 222/1 (b). Curves represent best nonlinear least-squares (NLLS) fit of variation of [CuBr₂] with time using a model curve of the form [CuBr₂] = AB_X(α + 1, 0) + c₀.

of MA initiated by MBP/Me₆TREN and activated copper wire. All polymerizations reached at least 80% conversion. The concentration data were obtained from the 957 nm absorbance¹ using the extinction coefficient of 460 M⁻¹ cm⁻¹ for CuBr₂/Me₆TREN in MA/DMSO mixtures.²⁹ Results obtained from analysis of Figure 1 are shown in Table 1.

Figure 1 presents several notable features. At both initiator concentrations, a greater total increase in [CuBr₂] was observed in polymerizations which were performed in the presence of initial added CuBr₂. This indicates that polymerizations carried out in the presence of additional deactivator paradoxically display lower retention of functionality, despite their lower dispersities and better adherence to the theoretical M_n vs conversion curve. At 80% conversion, polymerizations without CuBr₂ retained 98.7% (60/1 MA/MBP) or 98.4% (222/1 MA/MBP) of their functionality, while polymerizations with added

Table 1. Results of Analysis of CuBr₂ Kinetic Data During SET-LRP of MA¹

MA/MBP	60/1	60/1	222/1	222/1
added CuBr ₂	yes	no	yes	no
[MBP] ₀ (mM)	120	120	33	33
[CuBr ₂] ₀ (mM) ^a	0.76	0	0.43	0
final conversion (%)	80	95	90	95
Δ[CuBr ₂] (final conversion) (mM)	1.2	1.1	0.65	0.33
residual functionality at final conversion (mol %)	98	98	96	98
Δ[CuBr ₂] (80% conversion) (mM)	1.2	0.76	0.54	0.27
residual functionality (80% conversion) (mol %)	98.0	98.7	96.7	98.4
initial $d[\text{CuBr}_2]/dt$ ($\mu\text{M s}^{-1}$)	0.21 ^b	0.14 ^b	0.06 ^c	0.03 ^c
initial k_{a0} ($10^{-5} \text{ cm}\cdot\text{s}^{-1}$) ^d	4.30	2.40	3.82	2.00
$-d \ln[\text{MA}]/dt$ (10^{-4} s^{-1}) ^e	1.91	1.94	1.39	1.51
[R*] ^f (nM)	13.4	13.6	9.67	10.5
initial k_t ($10^8 \text{ L}\cdot\text{mol}^{-1}\cdot\text{s}^{-1}$)	11.7	7.6	6.5	2.7

^aCalculated using an extinction coefficient of $460 \text{ M}^{-1} \text{ s}^{-1}$.²⁹

^b $d[\text{CuBr}_2]/dt$ obtained from a linear fit of absorbance vs time data during initial 50 min of reaction. ^c $d[\text{CuBr}_2]/dt$ obtained from a linear fit of absorbance vs time data during initial 120 min of reaction. ^d $k_{a0} = (d[\text{CuBr}_2]/dt)/[\text{RBr}]/(\text{SA}_{\text{Cu}}/V)$; $\text{SA}_{\text{Cu}} = \pi(dl + d^2/2) = 0.074 \text{ cm}^2$, where $d = 0.0812 \text{ cm}$ and $l = 0.25 \text{ cm}$, reaction volume = 1.8 cm^3 . ^eData from reference 1. ^fCalculated assuming $k_p = 14300 \text{ L}\cdot\text{mol}^{-1}\cdot\text{s}^{-1}$.⁴⁵

CuBr₂ retained only 98.0% or 96.7%, respectively. These conclusions are in apparent conflict with an earlier study of retention of chain end functionality in SET-LRP, which found improved retention in the presence of CuBr₂ using high-resolution electrospray ionization mass spectrometry (ESI-MS).¹⁷ In that study, 96% retention of end group functionality was observed at near complete conversion for polymerizations without CuBr₂, compared to 98% in the presence of CuBr₂. However, a 50 min induction period was observed in polymerizations without CuBr₂, and 50% of the loss of functionality occurred during this time. If the induction period is excluded, similar results were obtained for polymerizations with and without CuBr₂. We would argue that UV-vis spectroscopy is a more sensitive and precise technique for probing small changes in end-group functionality than ESI-MS or NMR.

The polymerizations with added CuBr₂ also showed a higher initial rate of CuBr₂ production ($d[\text{CuBr}_2]/dt$). An approximate calculation of the initial k_{a0} , obtained by fitting a straight line to the first 50 (60/1 MA/MBP) or 120 (222/1 MA/MBP) minutes of the $[\text{CuBr}_2]$ vs time data, gives $4.1 \pm 0.3 \times 10^{-5} \text{ cm}\cdot\text{s}^{-1}$ (Table 1). When no CuBr₂ is added, the initial value of $d[\text{CuBr}_2]/dt$ is significantly lower, and k_{a0} values of $2.2 \pm 0.2 \times 10^{-5} \text{ cm}\cdot\text{s}^{-1}$ are obtained.

Finally, $d[\text{CuBr}_2]/dt$ decreases with time in all polymerizations. The decrease is too large to be explained by the change in $[\text{RBr}]$, which is <4%. It is most pronounced for the 60/1 MA/MBP polymerization in the presence of added CuBr₂.

All of these features can be explained by considering the effect of chain length on the rate of activation by copper metal. Longer chains react more slowly, either due to steric hindrance from the larger polymer chain or as a result of slower diffusion first of the whole chain, then of the halide terminus, to the copper surface. As a result, the rate constant for activation, k_{a0} , will show significant chain length dependence. In the presence of CuBr₂, the DP_n closely tracks the theoretical value, and

dispersity is low (~ 1.2) throughout the polymerization.¹ Without CuBr₂, the initial polymer produced is of much higher molecular weight (3500 and $7000 \text{ g}\cdot\text{mol}^{-1}$ for high and low $[\text{MBP}]_0$, respectively) and relatively polydisperse (>2). As a result, k_{a0} is initially lower in these polymerizations, resulting in lower rates of CuBr₂ generation and less loss of chain end functionality.

Differentiation of the $[\text{CuBr}_2]$ vs time data of Figures 1a and 1b reveals the relationship between k_{a0} and the degree of polymerization, DP_n (Figure 2). This was carried out by fitting

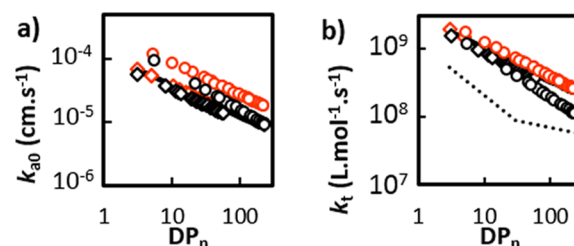


Figure 2. k_{a0} (a) and k_t (b) as a function of number-average degree of polymerization. Red: added CuBr₂. Black: No added CuBr₂. Diamonds: $[\text{MA}]_0/[\text{MBP}]_0 = 60/1$. Circles: $[\text{MA}]_0/[\text{MBP}]_0 = 222/1$. Model curves were obtained by NLLS fitting and represent (a) $k_{a0} = 1.25(9) \times 10^{-4} \text{ DP}_n^{-0.51(3)} \text{ cm}\cdot\text{s}^{-1}$ and (b) apparent $k_t = 3.1(1) \times 10^9 \text{ DP}_n^{-0.49(2)} \text{ L}\cdot\text{mol}^{-1}\cdot\text{s}^{-1}$. Dotted line represents the k_t of MA as measured by Buback et al.⁴⁶ using the SP-PLP-NIR-RAFT method.

the data for each set of polymerization conditions with a function of the form $[\text{CuBr}_2] = AB_X(\alpha + 1, 0) + c_0$, where $B_X(a, b)$ is the incomplete beta function and X is the conversion. Differentiation gives $d[\text{CuBr}_2]/dt = AX^\alpha$. As $d[\text{CuBr}_2]/dt$ is proportional to k_{a0} and X is proportional to DP_n , a simple change of scale gives k_{a0} as a function of DP_n . In the case of the 222/1 MA/MBP polymerization in the presence of CuBr₂, there appeared to be significant variation in the initial CuBr₂ concentration between experiments. As a result, these data were fitted to a function $[\text{CuBr}_2] = AB_X(\alpha + 1, 0) + c_i$ ($i = 1$ to 4), in which different c_i were used for each experiment. In all cases, excellent agreement was obtained between the raw data and the model curve. Full details of the fitting procedure, as well as estimates of error in the parameters, are given in the Supporting Information.

The different experiments give very similar results for k_{a0} as a function of DP_n , with the exception of the 222/1 MA/MBP polymerization in the presence of CuBr₂. This last experiment gives consistently higher values of k_{a0} , although with similar dependence on DP_n . A possible reason for this is the occurrence of a small amount of comproportionation, which will result in overestimation of k_{a0} , according to eq 13. Supporting this hypothesis, addition of a slow comproportionation reaction ($k_{\text{comp}} = 1.5 \times 10^{-6} \text{ cm}\cdot\text{s}^{-1}$) to the model brings all data into agreement without significantly affecting results of the high $[\text{MBP}]_0$ or low $[\text{CuBr}_2]_0$ polymerizations (see Supporting Information). After excluding the 222/1 MA/MBP polymerization in the presence of CuBr₂, the aggregated data are well described by a curve of the form $k_{a0} = 1.25(9) \times 10^{-4} \text{ DP}_n^{-0.51(3)} \text{ cm}\cdot\text{s}^{-1}$. For comparison, Peng et al. measured k_{a0} of MBP in 50/50 MA/DMSO to be $1.8 \times 10^{-4} \text{ cm}\cdot\text{s}^{-1}$ and k_{a0} of Br-terminated poly(methyl acrylate) to be $1.0 \times 10^{-4} \text{ cm}\cdot\text{s}^{-1}$.²⁹

The overall rate of polymerization, R_p , is given by $R_p = k_p[\text{MA}][\text{R}^*]$, and hence $-d(\ln[\text{MA}])/dt = k_p[\text{R}^*]$. All polymer-

izations displayed linear first-order kinetics, indicating that $k_p[R^*]$ was constant throughout the polymerization. As k_p is not expected to vary with chain length, $[R^*]$ must also be constant and is given by

$$[R^*] = \sqrt{\frac{k_{a0}[RBr]}{k_t}} = R_p/k_p \quad (16)$$

Thus, the ratio k_{a0}/k_t must also be approximately constant, indicating that k_t follows a similar chain length dependence to k_{a0} . This is plausible, as both reactions require the diffusion of large molecules and reaction between a large molecule and either a surface (activation) or another large molecule (termination). Significant chain-length-dependent steric effects will apply. Indeed the chain length dependence of k_t is well-known.^{46–50}

Approximate values for $[R^*]$ can be calculated using a value of 14300 L·mol⁻¹·s⁻¹ as the k_p of MA. It should be noted, however, that this value was determined in bulk MA⁴⁵ and may not be accurate for a polymerization carried out in the presence of 33% DMSO. Nevertheless, the $[R^*]$ obtained, which lies in the range 9–13 nM (Table 1), should be correct to within an order of magnitude. Notably, $[R^*]$ is virtually unaffected by the presence of $[CuBr_2]$, suggesting that the rate of comproportionation is negligible under these conditions. Estimates of the initial value of k_t for each reaction are in the vicinity of 10⁸–10⁹ L·mol⁻¹·s⁻¹, with higher values obtained for the 60/1 MA/MBP polymerizations (Table 1).

As for k_{a0} , k_t can be calculated at each stage of the polymerization by dividing $d[CuBr_2]/dt$ by $[R^*]^2$. In Figure 2b, k_t is plotted as a function of the theoretical degree of polymerization for each polymerization. Good agreement is obtained between the four separate experiments, although experiments without added $CuBr_2$ give generally lower values than those with added $CuBr_2$, particularly at higher DP_n . This may be a result of the higher dispersity polymer produced in these reactions and the poorer agreement between measured and theoretical DP_n . The production of high molecular weight polymer early in the reaction will result in more viscous solutions which will also depress k_t . The results are well described by a power law relationship of the form $k_t = k_t^{1,1} DP_n^{-\alpha}$, with the exponent α equal to 0.49(2) and $k_t^{1,1} = 3.1(1) \times 10^9$ L·mol⁻¹·s⁻¹.

Our calculated values of k_t are systematically higher than previously reported values obtained in bulk MA. This may be an effect of the solvent (DMSO), either directly on k_t or on k_p , which was used to estimate the radical concentration. Solvent effects on k_p of MA are, however, expected to be too small to explain the discrepancy.⁵¹ Another possibility is the occurrence of Cu-catalyzed radical termination, in which Cu(I) abstracts hydrogen from a propagating radical to form a Cu(II)–H species which can subsequently transfer hydrogen to another propagating radical to form dead polymer and regenerate Cu(I). This reaction has been shown to dominate the termination process under typical ATRP conditions, leading to loss of functionality which is an order of magnitude greater than that predicted from bimolecular radical termination alone.⁵² Despite these possible systematic errors in the magnitude of k_t , the overall dependence on DP_n is in reasonable agreement with the results of Buback et al.,⁴⁶ who found $k_t^{1,1}$ equal to 1.25×10^9 L·mol⁻¹·s⁻¹ and α equal to 0.78 for short chains ($DP_n < 30$) and 0.26 for long chains ($DP_n > 30$) using the SP-PLP-NIR-RAFT technique in bulk at 60 °C. The Percec

data set covers a DP_n range of 0–250 and thus spans both short and long chain regimes. We did not observe a significant difference in α between the low (MA/MBP = 60) and high (MA/MBP = 222) molecular weight polymerizations.

In conclusion, addition of deactivator in the form of $CuBr_2$ has the paradoxical effect of increasing the rate of termination and overall loss of chain end functionality, due to the generation of shorter polymer chains in the initial stages of the reaction which have higher rate constants of activation and termination. This suggests that in SET-LRP/SARA-ATRP, perhaps uniquely among reversible deactivation polymerizations, there is a trade-off between dispersity and chain end fidelity, with addition of deactivator improving the former at the expense of the latter. As for all radical polymerizations, reducing the rate of radical generation, for example by reducing the copper surface area or $[RBr]$, will increase chain end fidelity, while it will decrease in response to changes which increase the rate of radical generation. Termination occurs throughout the polymerization, but at a relatively low rate, leading to 1.3–3.3% loss of chain end functionality at 80% conversion. Thus, while SET-LRP/SARA-ATRP of MA may be a Methuselah among controlled radical polymerization techniques, it is not immortal. As J. M. Keynes pointed out,⁵³ in the long run we are all dead.

■ ASSOCIATED CONTENT

Supporting Information

Tabulated data, information on the NLLS fitting procedure, estimates of errors in the fitted parameters, and effect of a slow comproportionation reaction on the calculated values of k_{a0} . This material is available free of charge via the Internet at <http://pubs.acs.org>.

■ AUTHOR INFORMATION

Corresponding Author

*E-mail: harrisson@chimie.ups-tlse.fr

Notes

The authors declare no competing financial interest.

■ REFERENCES

- (1) Levere, M. E.; Nguyen, N. H.; Percec, V. *Macromolecules* **2012**, *45*, 8267–8274.
- (2) Jenkins, A. D.; Jones, R. G.; Moad, G. *Pure Appl. Chem.* **2010**, *82*, 483–491.
- (3) Rosen, B. M.; Percec, V. *Chem. Rev.* **2009**, *109*, 5069–5119.
- (4) Zhang, N.; Samanta, S. R.; Rosen, B. M.; Percec, V. *Chem. Rev.* **2014**, *114*, 5848–5958.
- (5) Konkolewicz, D.; Wang, Y.; Zhong, M.; Kryszewski, P.; Isse, A. A.; Gennaro, A.; Matyjaszewski, K. *Macromolecules* **2013**, *46*, 8749–8772.
- (6) Percec, V.; Popov, A. V.; Ramirez-Castillo, E.; Monteiro, M.; Barboiu, B.; Weichold, O.; Asandei, A. D.; Mitchell, C. M. *J. Am. Chem. Soc.* **2002**, *124*, 4940–4941.
- (7) Percec, V.; Guliasvili, T.; Ladislav, J. S.; Wistrand, A.; Stjern Dahl, A.; Sienkowska, M. J.; Monteiro, M. J.; Sahoo, S. *J. Am. Chem. Soc.* **2006**, *128*, 14156–14165.
- (8) Jiang, X.; Rosen, B. M.; Percec, V. *J. Polym. Sci., Part A: Polym. Chem.* **2010**, *48*, 2716–2721.
- (9) Nguyen, N. H.; Levere, M. E.; Percec, V. *J. Polym. Sci., Part A: Polym. Chem.* **2012**, *50*, 860–873.
- (10) Lligadas, G.; Rosen, B. M.; Bell, C. A.; Monteiro, M. J.; Percec, V. *Macromolecules* **2008**, *41*, 8365–8371.
- (11) Nguyen, N. H.; Sun, H. J.; Levere, M. E.; Fleischmann, S.; Percec, V. *Polym. Chem.* **2013**, *4*, 1328–1332.
- (12) Lligadas, G.; Percec, V. *J. Polym. Sci., Part A: Polym. Chem.* **2007**, *45*, 4684–4695.

- (13) Lligadas, G.; Percec, V. *J. Polym. Sci., Part A: Polym. Chem.* **2008**, *46*, 2745–2754.
- (14) Lligadas, G.; Rosen, B. M.; Monteiro, M. J.; Percec, V. *Macromolecules* **2008**, *41*, 8360–8364.
- (15) Anastasaki, A.; Waldron, C.; Wilson, P.; Boyer, C.; Zetterlund, P. B.; Whittaker, M. R.; Haddleton, D. *ACS Macro Lett.* **2013**, *2*, 896–900.
- (16) Boyer, C.; Soeriyadi, A. H.; Zetterlund, P. B.; Whittaker, M. R. *Macromolecules* **2011**, *44*, 8028–8033.
- (17) Nyström, F.; Soeriyadi, A. H.; Boyer, C.; Zetterlund, P. B.; Whittaker, M. R. *J. Polym. Sci., Part A: Polym. Chem.* **2011**, *49*, 5313–5321.
- (18) Soeriyadi, A. H.; Boyer, C.; Nyström, F.; Zetterlund, P. B.; Whittaker, M. R. *J. Am. Chem. Soc.* **2011**, *133*, 11128–11131.
- (19) Nguyen, N. H.; Levere, M. E.; Kulis, J.; Monteiro, M. J.; Percec, V. *Macromolecules* **2012**, *45*, 4606–4622.
- (20) Bell, C. A.; Jia, Z.; Kulis, J.; Monteiro, M. J. *Macromolecules* **2011**, *44*, 4814–4827.
- (21) Kulis, J.; Jia, Z.; Monteiro, M. J. *Macromolecules* **2012**, *45*, 5956–5966.
- (22) Kulis, J.; Bell, C. A.; Micallef, A. S.; Monteiro, M. J. *J. Polym. Sci., Part A: Polym. Chem.* **2010**, *48*, 2214–2223.
- (23) Kulis, J.; Bell, C. A.; Micallef, A. S.; Monteiro, M. J. *Aust. J. Chem.* **2010**, *63*, 1227–1236.
- (24) Kulis, J.; Bell, C. A.; Micallef, A. S.; Jia, Z.; Monteiro, M. J. *Macromolecules* **2009**, *42*, 8218–8227.
- (25) Jia, Z.; Bell, C. A.; Monteiro, M. J. *Macromolecules* **2011**, *44*, 1747–1751.
- (26) Jia, Z.; Bell, C. A.; Monteiro, M. J. *Chem. Commun.* **2011**, *47*, 4165–4167.
- (27) Konkolewicz, D.; Krys, P.; Góis, J. R.; Mendonça, P. V.; Zhong, M.; Wang, Y.; Gennaro, A.; Isse, A. A.; Fantin, M.; Matyjaszewski, K. *Macromolecules* **2014**, *47*, 560–570.
- (28) Konkolewicz, D.; Wang, Y.; Zhong, M.; Krys, P.; Isse, A. A.; Gennaro, A.; Matyjaszewski, K. *Macromolecules* **2013**, *46*, 8749–8772.
- (29) Peng, C. H.; Zhong, M.; Wang, Y.; Kwak, Y.; Zhang, Y.; Zhu, W.; Tonge, M.; Buback, J.; Park, S.; Krys, P.; Konkolewicz, D.; Gennaro, A.; Matyjaszewski, K. *Macromolecules* **2013**, *46*, 3803–3815.
- (30) Wang, Y.; Zhong, M.; Zhu, W.; Peng, C. H.; Zhang, Y.; Konkolewicz, D.; Bortolamei, N.; Isse, A. A.; Gennaro, A.; Matyjaszewski, K. *Macromolecules* **2013**, *46*, 3793–3802.
- (31) Zhang, Y.; Wang, Y.; Peng, C. H.; Zhong, M.; Zhu, W.; Konkolewicz, D.; Matyjaszewski, K. *Macromolecules* **2011**, *45*, 78–86.
- (32) Zhong, M.; Wang, Y.; Krys, P.; Konkolewicz, D.; Matyjaszewski, K. *Macromolecules* **2013**, *46*, 3816–3827.
- (33) Abreu, C. M.; Serra, A. C.; Popov, A. V.; Matyjaszewski, K.; Guliashvili, T.; Coelho, J. F. *Polym. Chem.* **2013**, *4*, 5629–5636.
- (34) Abreu, C. M.; Mendonça, P. V.; Serra, A. C.; Popov, A. V.; Matyjaszewski, K.; Guliashvili, T.; Coelho, J. F. *ACS Macro Lett.* **2012**, *1*, 1308–1311.
- (35) Matyjaszewski, K.; Tsarevsky, N. V.; Braunecker, W. A.; Dong, H.; Huang, J.; Jakubowski, W.; Kwak, Y.; Nicolay, R.; Tang, W.; Yoon, J. A. *Macromolecules* **2007**, *40*, 7795–7806.
- (36) Guliashvili, T.; Mendonça, P. V.; Serra, A. C.; Popov, A. V.; Coelho, J. F. *J. Chem.—Eur. J.* **2012**, *18*, 4607–4612.
- (37) Konkolewicz, D.; Wang, Y.; Krys, P.; Zhong, M.; Isse, A. A.; Gennaro, A.; Matyjaszewski, K. *Polym. Chem.* **2014**.
- (38) De Paoli, P.; Isse, A. A.; Bortolamei, N.; Gennaro, A. *Chem. Commun.* **2011**, *47*, 3580–3582.
- (39) Harrisson, S.; Couvreur, P.; Nicolas, J. *Macromolecules* **2012**, *45*, 7388–7396.
- (40) Hornby, B. D.; West, A. G.; Tom, J. C.; Waterson, C.; Harrisson, S.; Perrier, S. *Macromol. Rapid Commun.* **2010**, *31*, 1276–1280.
- (41) Tom, J.; Hornby, B.; West, A.; Harrisson, S.; Perrier, S. *Polym. Chem.* **2010**, *1*, 420–422.
- (42) West, A. G.; Hornby, B.; Tom, J.; Admiral, V.; Harrisson, S.; Perrier, S. *Macromolecules* **2011**, *44*, 8034–8041.
- (43) Matyjaszewski, K. *Macromolecules* **2012**, *45*, 4015–4039.
- (44) Wang, Y.; Zhong, M.; Zhang, Y.; Magenau, A. J. D.; Matyjaszewski, K. *Macromolecules* **2012**, *45*, 8929–8932.
- (45) Junkers, T.; Schneider-Baumann, M.; Koo, S. S. P.; Castignolles, P.; Barner-Kowollik, C. *Macromolecules* **2010**, *43*, 10427–10434.
- (46) Buback, M.; Hesse, P.; Junkers, T.; Theis, T.; Vana, P. *Aust. J. Chem.* **2007**, *60*, 779–787.
- (47) Barth, J.; Buback, M.; Russell, G. T.; Smolne, S. *Macromol. Chem. Phys.* **2011**, *212*, 1366–1378.
- (48) Buback, M.; Egorov, M.; Feldermann, A. *Macromolecules* **2004**, *37*, 1768–1776.
- (49) Theis, A.; Feldermann, A.; Charton, N.; Stenzel, M. H.; Davis, T. P.; Barner-Kowollik, C. *Macromolecules* **2005**, *38*, 2595–2605.
- (50) Johnston-Hall, G.; Monteiro, M. J. *J. Polym. Sci., Part A: Polym. Chem.* **2008**, *46*, 3155–3173.
- (51) Wang, Y.; Kwak, Y.; Buback, J.; Buback, M.; Matyjaszewski, K. *ACS Macro Lett.* **2012**, *1*, 1367–1370.
- (52) Wang, Y.; Soerensen, N.; Zhong, M.; Schroeder, H.; Buback, M.; Matyjaszewski, K. *Macromolecules* **2013**, *46*, 683–691.
- (53) Keynes, J. M. *A Tract on Monetary Reform*; Macmillan and Co., Ltd.: London, 1923.